Scientia Iranica B (2014) 21(3), 587–599

SCIENTIA IRANICA

Sharif University of Technology
Scientia Iranica
Transactions B: Mechanical Engineering
www.scientiairanica.com

Investigation of the dynamic behavior of thick piezoelectric cylinders

H. Rajabi[a,*] and A. Darvizeh[b]

a. *Department of Mechanical Engineering, Ahrar Institute of Technology and Higher Education, Rasht, Iran.*
b. *Department of Mechanical Engineering, Faculty of Engineering, Anzali Branch, Islamic Azad University, Bandar Anzali, Iran.*

Received 3 September 2012; received in revised form 27 October 2013; accepted 24 December 2013

KEYWORDS
Theoretical solution;
Piezoelectric shell;
FSDT;
Navier solution;
Dynamic load.

Abstract. A theoretical solution of the mechanical behavior of thick piezoelectric cylinders subjected to dynamic pressures is presented in this paper. The five governing equations in terms of resultant forces and resultant moments with respect to basic displacement vector components , and are used. The First-order Shear Deformation Theory (FSDT) is employed to consider the effects of shear forces on the shell structure. The effects of transverse shear deformation and rotary inertia are included into the analysis. The formulation is based on the thick-shell equations. Navier-type solutions are obtained and used for simply supported circular cylindrical shells. Finally, the Newmark family of methods is used to numerically time integration of the system of coupled second order ODEs. Results obtained with the present analysis are found to be in good agreement with those available in the literature. The results of this paper can serve as a reference for future study in the design of smart engineering structures

1. Introduction

In recent years, piezoelectric cylindrical shells have attracted significant attention in both academic and industrial fields. They are widely used in modern industries, such as electronics, biotechnology, aerospace, automotive, and so on.

From a historical point of view, fundamental theories for the modeling of the piezoelectric structures were fully developed by Tiersten [1]. Tzou and Zhong [2] derived system equations for piezoelectric thin shell vibrations. Hamilton's principle and the linear piezoelectricity theory were used in this work to derive the general piezoelastic system equations of piezoelectric shells. Lee [3] and Tzou [4] gave us both a piezoelectric plate theory and a piezoelectric shell theory based on the classical plate and shell theory, respectively. The effectiveness of piezoelectric sensors and actuators, laminated on simply supported rectangular thin plates and circular cylindrical thin shells, using the Classical Laminate Theory (CLT), was investigated by Tzou and Fu [5,6] and Tzou et al. [7,8]. Pinto Correia et al. [9] developed a semi-analytical piezoelectric shell model for vibration control of the structure. A mixed finite element approach was used, which combined the equivalent single-layer higher order shear deformation theory, to represent the mechanical behavior of the shell. Kapuria et al. [10-12] introduced a 3D piezoelectric solution for simply supported laminated circular cylindrical shells under electro-mechanical loads. 3D exact solutions have been given by Ray et al. [13] and Dube et al. [14] for piezoelectric simply supported plates under thermo-electro-mechanical loads. Chen et al. [15] presented an exact elasticity solution for an orthotropic cylindrical shell with piezoelectric layers. Stress and displacement distributions subjected to static mechanical and electrical loading have been given in this paper. An exact 3D

*. *Corresponding author. Tel: +98 911 338 5460*
E-mail addresses: harajabi@hotmail.com (H. Rajabi); adarvizeh@guilan.ac.ir (A. Darvizeh)

solution for the static behavior of a simply supported laminated piezoelectric cylinder can be found in the work of Heyliger [16]. The Frobenius method has been used to obtain the elastic and electrical fields for each layer. A nonlinear finite element solution was proposed by authors and co-workers [17] for multi-layer piezoelectric structures considering large deformation effects. The virtual work principle and the Lagrangian Update Method (LUM) were employed in this study. Shakeri et al. [18] presented the elasticity solution for an infinitely long, simply supported, orthotropic, piezoelectric cylindrical shell panel under dynamic pressure. Darvizeh et al. [19] carried out a study on the effects of piezoelectric layers on the buckling behavior of a composite cylinder. Recently, a three dimensional analysis of orthotropic thick-walled tubes coated with piezoelectric sensors and actuators was carried out using analytical methods and numerical modeling [20]. Another theoretical method was developed by authors and co-authors to determine the dynamic response of piezoelectric circular cylindrical shells subjected to internal loading [21]. An approximate solution was obtained using the Galerkin method.

In recent years, a variety of computational solutions has been presented for piezoelectric shells by Hong [22], Kumar et al. [23], Klinkel and Wagner [24], Santos et al. [25,26], Deu et al. [27], etc.

In the present work, particular attention is devoted to the modeling of thick circular cylindrical shells covered with piezoelectric layers under internal dynamic loading using an analytical solution. The word "thick" means that the effect of factor $(1+\frac{z}{R})$ is considered in calculating resultant forces and resultant moments. This factor results from the trapezoid-like shape of the cross-section of the shell and is usually neglected in the thin shell theory [28]. Theoretical formulations, based on FSDT, take into consideration transverse shear deformation and rotary inertia effects. The formulation is general. Analytical results for a piezoelectric shell with simply supported boundary conditions are based on the Navier solution method. The Newmark family of methods is used for the numerical time integration of the system of coupled second order Ordinary Differential Equations (ODEs). In some cases, in order to prove the validity of the presented method and the solving process, a dynamic numerical solution for the same example is given. Comparing the results of the presented method with those obtained by numerical solutions, shows that the presented method is effective and accurate.

2. Governing equations

2.1. Equations of motion

A three-dimensional elastic body is enclosed by two neighborhoods or closely curved surfaces called the "shell". The distance between these two surfaces defines the thickness of the shell. The "mid-surface" of the shell is a surface passing through the mid-thickness at each point [29]. It means that, in a circular cylinder of radius R, the mid-surface is a minimal surface with the radii of curvature R, and is infinite along the radial and axial directions, respectively. If the thickness of the shell is small, compared with the other dimensions, then, the shell is considered "thin"; otherwise, the shell is "thick".

Consider a thick-walled circular cylinder made up of a linear orthotropic material with surfaces bonded by piezoelectric layers, with poling in the z direction (Figure 1). The orthogonal coordinate system (x, ϑ, z) is fixed at the mid-surface of the tube with length, L, thickness, H, and radius, R. x is the axial direction, ϑ is the circumferential direction and z is the radial direction. The deformations of the tube are defined by u, v, w, which are displacements of the point in x, ϑ, z.

The stress analysis on the sides of an element of the shell structure is shown in Figure 2. For the mid-surface, we defined the six force $(N_x, N_\vartheta, N_{x\vartheta}, N_{\vartheta x}, Q_x, Q_\vartheta)$ and four moment $(M_x, M_\vartheta, M_{x\vartheta}, M_{\vartheta x})$ resultants, and the distributed load consisting of three forces (P_x, P_ϑ, P_z) and two moments (m_x, m_ϑ). The governing equations of motion in the longitudinal, tangential and radial directions, in terms of force and moment resultants, are as follows [28]:

$$N_{x,x}+\frac{N_{\vartheta x,\vartheta}}{R}+P_x=I_0\ddot{u}_0+I_1\ddot{\varphi}_x,$$

$$N_{x\vartheta,x}+\frac{N_{\vartheta,\vartheta}}{R}+\frac{Q_\vartheta}{R}+P_\vartheta=I_0\ddot{v}_0+I_1\ddot{\varphi}_\vartheta,$$

$$Q_{x,x}+\frac{Q_{\vartheta,\vartheta}}{R}-\frac{N_\vartheta}{R}+P_z=I_0\ddot{w}_0,$$

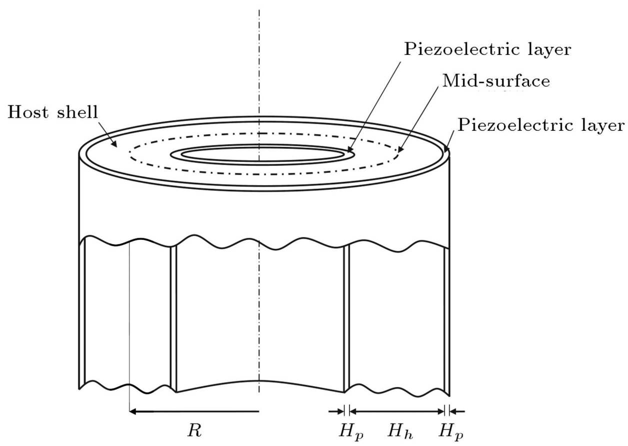

Figure 1. Circular cylindrical shell with piezoelectric layers at surfaces. R, H_p and H_h are mid-surface radius, thickness of the piezoelectric layers and thickness of the host shell, respectively.

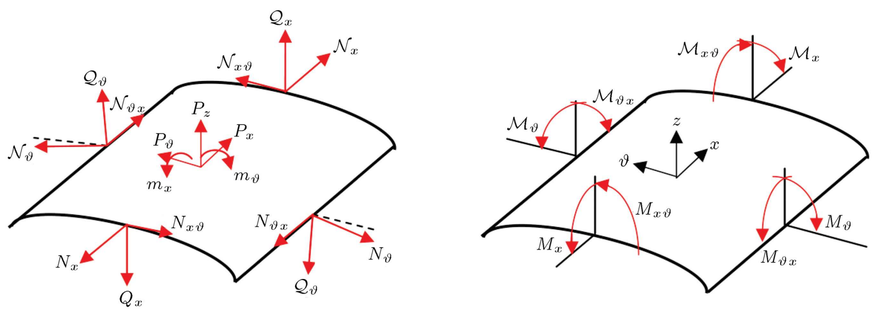

$$\mathcal{N}_x = N_x + \frac{\partial N_x}{\partial x}dx \qquad \mathcal{M}_x = M_x + \frac{\partial M_x}{\partial x}dx$$

$$\mathcal{N}_\vartheta = N_\vartheta + \frac{\partial N_\vartheta}{\partial \vartheta}d\vartheta \qquad \mathcal{M}_\vartheta = M_\vartheta + \frac{\partial M_\vartheta}{\partial \vartheta}d\vartheta \qquad \mathcal{Q}_x = Q_x + \frac{\partial Q_x}{\partial x}dx$$

$$\mathcal{N}_{x\vartheta} = N_{x\vartheta} + \frac{\partial N_{x\vartheta}}{\partial x}dx \qquad \mathcal{M}_{x\vartheta} = M_{x\vartheta} + \frac{\partial M_{x\vartheta}}{\partial x}dx \qquad \mathcal{Q}_\vartheta = Q_\vartheta + \frac{\partial Q_\vartheta}{\partial \vartheta}d\vartheta$$

$$\mathcal{N}_{\vartheta x} = N_{\vartheta x} + \frac{\partial N_{\vartheta x}}{\partial \vartheta}d\vartheta \qquad \mathcal{M}_{\vartheta x} = M_{\vartheta x} + \frac{\partial M_{\vartheta x}}{\partial \vartheta}d\vartheta$$

Figure 2. The forces and moments acting on the sides of an element of the circular cylindrical shell.

$$M_{x,x} + \frac{M_{\vartheta x,\vartheta}}{R} - Q_x + m_x = I_1\ddot{u}_0 + I_2\ddot{\varphi}_x,$$

$$M_{x\vartheta,x} + \frac{M_{\vartheta,\vartheta}}{R} - Q_\vartheta + m_\vartheta = I_1\ddot{v}_0 + I_2\ddot{\varphi}_\vartheta, \tag{1}$$

the mass moments of inertia are:

$$I_0 = \int_{-\frac{H}{2}}^{\frac{H}{2}} \rho\left(1+\frac{z}{R}\right)dz, \qquad I_1 = \int_{-\frac{H}{2}}^{\frac{H}{2}} \rho z\left(1+\frac{z}{R}\right)dz,$$

$$I_2 = \int_{-\frac{H}{2}}^{\frac{H}{2}} \rho z^2\left(1+\frac{z}{R}\right)dz, \tag{2}$$

and ρ is the density of the shell.

The force and moment resultants that act on a shell element are defined as the force and moment per unit length of the shell's mid-surface. The resultants, which are obtained by integrating the stresses acting on differential area elements of a shell element, have the following definitions:

$$N_x = \int_{-\frac{H}{2}}^{\frac{H}{2}} \sigma_x\left(1+\frac{z}{R}\right)dz, \qquad N_\vartheta = \int_{-\frac{H}{2}}^{\frac{H}{2}} \sigma_\vartheta dz,$$

$$N_{x\vartheta} = \int_{-\frac{H}{2}}^{\frac{H}{2}} \sigma_{x\vartheta}\left(1+\frac{z}{R}\right)dz, \qquad N_{\vartheta x} = \int_{-\frac{H}{2}}^{\frac{H}{2}} \sigma_{\vartheta x} dz,$$

$$M_x = \int_{-\frac{H}{2}}^{\frac{H}{2}} \sigma_x\left(1+\frac{z}{R}\right)zdz, \qquad M_\vartheta = \int_{-\frac{H}{2}}^{\frac{H}{2}} \sigma_\vartheta zdz,$$

$$M_{x\vartheta} = \int_{-\frac{H}{2}}^{\frac{H}{2}} \sigma_{x\vartheta}\left(1+\frac{z}{R}\right)zdz, \qquad M_{\vartheta x} = \int_{-\frac{H}{2}}^{\frac{H}{2}} \sigma_{\vartheta x} zdz,$$

$$Q_x = \int_{-\frac{H}{2}}^{\frac{H}{2}} \sigma_{zx}\left(1+\frac{z}{R}\right)dz, \qquad Q_\vartheta = \int_{-\frac{H}{2}}^{\frac{H}{2}} \sigma_{\vartheta z} dz, \tag{3}$$

where $\sigma_x, \sigma_\vartheta, \sigma_{x\vartheta}, \sigma_{zx}$ and $\sigma_{\vartheta z}$ are the normal and shear stresses distributed in the shell.

Note that, for a thick shell, the term $(\frac{z}{R})$ in the force and moment resultants is so large that it cannot be neglected.

2.2. Constitutive equations

2.2.1. Host shell

Plates and shells with complex shapes made of orthotropic materials are widely used for the construction of structure elements in modern engineering [30]. The mechanical constitutive equations, which relate the stresses to the strains, for this kind of material, can be written as:

$$\begin{pmatrix} \sigma_x \\ \sigma_\theta \\ \sigma_z \\ \tau_{\theta z} \\ \tau_{xz} \\ \tau_{x\theta} \end{pmatrix} = \begin{pmatrix} Q_{11} & Q_{12} & Q_{13} & 0 & 0 & 0 \\ Q_{21} & Q_{22} & Q_{23} & 0 & 0 & 0 \\ Q_{31} & Q_{32} & Q_{33} & 0 & 0 & 0 \\ 0 & 0 & 0 & Q_{44} & 0 & 0 \\ 0 & 0 & 0 & 0 & Q_{55} & 0 \\ 0 & 0 & 0 & 0 & 0 & Q_{66} \end{pmatrix}$$

$$\begin{pmatrix} \varepsilon_x \\ \varepsilon_\theta \\ \varepsilon_z \\ \gamma_{\theta z} \\ \gamma_{xz} \\ \gamma_{x\theta} \end{pmatrix}. \tag{4}$$

Q is the stiffness matrix and its elements are:

$$Q_{11}=\frac{E_{11}}{D_0}(1-v_{23}v_{32}),$$

$$Q_{12}=\frac{E_{11}}{D_0}(v_{21}+v_{23}v_{31}),$$

$$Q_{13}=\frac{E_{11}}{D_0}(v_{21}v_{32}+v_{31}),$$

$$Q_{22}=\frac{E_{22}}{D_0}(1-v_{13}v_{31}),$$

$$Q_{23}=\frac{E_{22}}{D_0}(v_{32}+v_{12}v_{31}),$$

$$Q_{33}=\frac{E_{33}}{D_0}(1-v_{12}v_{21}),$$

$$Q_{21}=Q_{12}, \qquad Q_{31}=Q_{13},$$

$$Q_{32}=Q_{23}, \qquad Q_{44}=G_{23},$$

$$Q_{55}=G_{13}, \qquad Q_{66}=G_{12}. \tag{5}$$

D_0 may be written as:

$$D_0=1-v_{12}v_{21}-v_{13}v_{31}-v_{23}v_{32}-v_{12}v_{23}v_{31}-v_{13}v_{21}v_{32}. \tag{6}$$

In the above equations, E_{ii} is referred to as Young's modulus, G_{ij} as the elastic shear modulus and v_{ij} as Poisson's ratio.

2.2.2. Piezoelectric layers

The linear constitutive equations of a linear piezoelectric material in the general case of an arbitrary state of stress are given by Ikeda [31]:

$$\begin{pmatrix}\sigma_x\\ \sigma_\theta\\ \sigma_z\\ \tau_{\theta z}\\ \tau_{xz}\\ \tau_{x\theta}\end{pmatrix}=\begin{pmatrix}C_{11}&C_{12}&C_{13}&0&0&0\\ C_{21}&C_{22}&C_{23}&0&0&0\\ C_{31}&C_{32}&C_{33}&0&0&0\\ 0&0&0&C_{44}&0&0\\ 0&0&0&0&C_{55}&0\\ 0&0&0&0&0&C_{66}\end{pmatrix}\begin{pmatrix}\varepsilon_x\\ \varepsilon_\vartheta\\ \varepsilon_z\\ \gamma_{\vartheta z}\\ \gamma_{xz}\\ \gamma_{x\vartheta}\end{pmatrix}-\begin{pmatrix}0&0&e_{31}\\ 0&0&e_{32}\\ 0&0&e_{33}\\ 0&e_{24}&0\\ e_{15}&0&0\\ 0&0&0\end{pmatrix}\begin{pmatrix}\mathbb{E}_x\\ \mathbb{E}_\vartheta\\ \mathbb{E}_z\end{pmatrix}, \tag{7}$$

$$\begin{pmatrix}D_x\\ D_\vartheta\\ D_z\end{pmatrix}=\begin{pmatrix}0&0&0&0&e_{15}&0\\ 0&0&0&e_{24}&0&0\\ e_{31}&e_{32}&e_{33}&0&0&0\end{pmatrix}\begin{pmatrix}\varepsilon_x\\ \varepsilon_\vartheta\\ \varepsilon_z\\ \gamma_{\vartheta z}\\ \gamma_{xz}\\ \gamma_{x\vartheta}\end{pmatrix}+\begin{pmatrix}\eta_{11}&0&0\\ 0&\eta_{22}&0\\ 0&0&\eta_{33}\end{pmatrix}\begin{pmatrix}\mathbb{E}_x\\ \mathbb{E}_\vartheta\\ \mathbb{E}_z\end{pmatrix}, \tag{8}$$

where the matrices, C, e and η, respectively, denote the elastic stiffness, and the piezoelectric and dielectric constants of the piezoelectric layers. Also, D and $\mathbb{E}$ are the electric displacement and the electric field vectors, respectively.

Piezoelectric layers are polarized along the radial direction. Then:

$$\mathbb{E}_x=0, \tag{9}$$

$$\mathbb{E}_\vartheta=0\ . \tag{10}$$

$\mathbb{E}_z$ can be expressed as summation of two parameters:

$$\mathbb{E}_z=\mathbb{E}'_z+\mathbb{E}''_z, \tag{11}$$

where $\mathbb{E}'_z$ is the electric field, due to applied actuation potentials, and $\mathbb{E}''_z$ is the electric field due to direct piezoelectric effects. Using Eq. (8), for electric displacement along the radial direction, we have:

$$D_z=(e_{31}\varepsilon_x+e_{32}\varepsilon_\vartheta+e_{33}\varepsilon_z+\eta_{33}\mathbb{E}''_z)+\eta_{33}\mathbb{E}'_z. \tag{12}$$

In the bracket, the expression can be constrained to be zero because its value is small compared to the last term [32]. Hence:

$$\mathbb{E}''_z=-\frac{1}{\eta_{33}}(e_{31}\varepsilon_x+e_{32}\varepsilon_\vartheta+e_{33}\varepsilon_z). \tag{13}$$

Then, using Eqs. (11) and (13), we can write:

$$\mathbb{E}_z=\mathbb{E}'_z-\frac{1}{\eta_{33}}(e_{31}\varepsilon_x+e_{32}\varepsilon_\vartheta+e_{33}\varepsilon_z). \tag{14}$$

In this investigation, it is assumed that the interface between the piezoelectric layer and the host structure are perfectly bonded. As we know, in application, if a piezoelectric material is selected to be an actuator, due to its significantly large rigidity, the length of the actuator should be small enough to conform to the perfect bond assumption [33]. The assumption may cause an error of up to 8% in the predicted deflection compared to the experimental results [34].

2.3. Compatibility equations

The strain-displacement equations for a thick cylindrical shell are given by Eqs. (15):

$$\begin{aligned}
&\varepsilon_x = u_{,x},\\
&\varepsilon_\vartheta = (v_{,\vartheta} + w)/(R+z),\\
&\varepsilon_z = w_{,z},\\
&\gamma_{\vartheta z} = (w_{,\vartheta} - v)/(R+z) + \varphi_\vartheta,\\
&\gamma_{xz} = \varphi_x + w_{,x},\\
&\gamma_{x\vartheta} = u_{,\vartheta}/(R+z) + v_{,x}.
\end{aligned} \tag{15}$$

As mentioned before, u, v, w are the displacements along x, ϑ and z axes, respectively; φ_x and φ_ϑ are angles of rotation of the cross-sections that were normal to the mid-surface of the unformed shell.

2.4. FSDT

The first-order shear deformation theory is used to deal with the influence of shear forces on the deformation of the shell. In the first-order shear deformation, the Kirchhoff hypothesis is relaxed by not constraining the transverse normals to remain perpendicular to the mid-surface after deformation [35]. This amounts to including transverse shear strains in the theory. The inextensibility of transverse normals requires that w be independent of the thickness coordinate.

According to the first-order shear deformation theory, the displacements are of the form:

$$\begin{aligned}
&u(x,\vartheta,z,t) = u_0(x,\vartheta,t) + z\varphi_x(x,\vartheta,t),\\
&v(x,\vartheta,z,t) = v_0(x,\vartheta,t) + z\varphi_\vartheta(x,\vartheta,t),\\
&w(x,\vartheta,z,t) = w_0(x,\vartheta,t),
\end{aligned} \tag{16}$$

where u_0, v_0, w_0, φ_x and φ_ϑ are unknowns to be determined.

In fact, u_0, v_0, w_0, φ_x and φ_ϑ are the displacements of a point on the surface, $z = 0$, and the rotations of transverse normal about its ϑ and x axes, respectively.

Substituting Eqs. (16) into Eqs. (15) yields:

$$\begin{aligned}
&\varepsilon_x = u_{0,x} + z\varphi_{x,x},\\
&\varepsilon_\vartheta = (v_{0,\vartheta} + z\varphi_{\vartheta,\vartheta} + w_0)/(R+z),\\
&\varepsilon_z = 0,\\
&\gamma_{\vartheta z} = (w_{0,\vartheta} - v_0 - z\varphi_\vartheta)/(R+z) + \varphi_\vartheta,\\
&\gamma_{xz} = \varphi_x + w_{0,x},\\
&\gamma_{x\vartheta} = (u_{0,\vartheta} + z\varphi_{x,\vartheta})/(R+z) + v_{0,x} + z\varphi_{\vartheta,x}.
\end{aligned} \tag{17}$$

Substituting Eqs. (17) into Eqs. (4) and (7), using the obtained equations in Eqs. (3), results:

$$\begin{aligned}
N_x =& \left(A_{11} + \frac{B_{11}}{R}\right) u_{0,x} + \left(\frac{A_{12}}{R}\right) v_{0,\vartheta}\\
&+ \left(\frac{A_{12}}{R}\right) w_0 + \left(B_{11} + \frac{C_{11}}{R}\right) \varphi_{x,x}\\
&+ \left(\frac{B_{12}}{R}\right) \varphi_{\vartheta,\vartheta} + N_x^*,
\end{aligned}$$

$$\begin{aligned}
N_\vartheta =& (A_{12}) u_{0,x} + \left(\frac{A_{22}}{R} - \frac{B_{22}}{R^2} + \frac{C_{22}}{R^3}\right) v_{0,\vartheta}\\
&+ \left(\frac{A_{22}}{R} - \frac{B_{22}}{R^2} + \frac{C_{22}}{R^3}\right) w_0 + (B_{12})\varphi_{x,x}\\
&+ \left(\frac{B_{22}}{R} - \frac{C_{22}}{R^2} + \frac{D_{22}}{R^3}\right) \varphi_{\vartheta,\vartheta} + N_\vartheta^*,
\end{aligned}$$

$$\begin{aligned}
N_{x\vartheta} =& \left(\frac{A_{66}}{R}\right) u_{0,\vartheta} + \left(A_{66} + \frac{B_{66}}{R}\right) v_{0,x}\\
&+ \left(\frac{B_{66}}{R}\right) \varphi_{x,\vartheta} + \left(B_{66} + \frac{C_{66}}{R}\right) \varphi_{\vartheta,x},
\end{aligned}$$

$$\begin{aligned}
N_{\vartheta x} =& \left(\frac{A_{66}}{R} - \frac{B_{66}}{R^2} + \frac{C_{66}}{R^3}\right) u_{0,\vartheta}\\
&+ (A_{66}) v_{0,x} + \left(\frac{B_{66}}{R} - \frac{C_{66}}{R^2} + \frac{D_{66}}{R^3}\right) \varphi_{x,\vartheta}\\
&+ (B_{66})\varphi_{\vartheta,x},
\end{aligned}$$

$$\begin{aligned}
M_x =& \left(B_{11} + \frac{C_{11}}{R}\right) u_{0,x} + \left(\frac{B_{12}}{R}\right) v_{0,\vartheta} + \left(\frac{B_{12}}{R}\right) w_0\\
&+ \left(C_{11} + \frac{D_{11}}{R}\right) \varphi_{x,x} + \left(\frac{C_{12}}{R}\right) \varphi_{\vartheta,\vartheta} + M_x^*,
\end{aligned}$$

$$\begin{aligned}
M_\vartheta =& (B_{12}) u_{0,x} + \left(\frac{B_{22}}{R} - \frac{C_{22}}{R^2} + \frac{D_{22}}{R^3}\right) v_{0,\vartheta}\\
&+ \left(\frac{B_{22}}{R} - \frac{C_{22}}{R^2} + \frac{D_{22}}{R^3}\right) w_0 + (C_{12})\varphi_{x,x}\\
&+ \left(\frac{C_{22}}{R} - \frac{D_{22}}{R^2} + \frac{E_{22}}{R^3}\right) \varphi_{\vartheta,\vartheta} + M_\vartheta^*,
\end{aligned}$$

$$\begin{aligned}
M_{x\vartheta} =& \left(\frac{B_{66}}{R}\right) u_{0,\vartheta} + \left(B_{66} + \frac{C_{66}}{R}\right) v_{0,x}\\
&+ \left(\frac{C_{66}}{R}\right) \varphi_{x,\vartheta} + \left(C_{66} + \frac{D_{66}}{R}\right) \varphi_{\vartheta,x},
\end{aligned}$$

$$M_{\vartheta x}=\left(\frac{B_{66}}{R}-\frac{C_{66}}{R^2}+\frac{D_{66}}{R^3}\right)u_{0,\vartheta}+(B_{66})v_{0,x}$$
$$+\left(\frac{C_{66}}{R}-\frac{D_{66}}{R^2}+\frac{E_{66}}{R^3}\right)\varphi_{x,\vartheta}+(C_{66})\varphi_{\vartheta,x},$$
$$Q_x=\left(A_{55}+\frac{B_{55}}{R}\right)w_{0,x}+\left(A_{55}+\frac{B_{55}}{R}\right)\varphi_x+Q_x^*,$$
$$Q_\vartheta=-\left(\frac{A_{44}}{R}-\frac{B_{44}}{R^2}+\frac{C_{44}}{R^3}\right)v_0$$
$$+\left(\frac{A_{44}}{R}-\frac{B_{44}}{R^2}+\frac{C_{44}}{R^3}\right)w_{0,\vartheta}$$
$$+\left(A_{44}-\frac{B_{44}}{R}+\frac{C_{44}}{R^2}\right)\varphi_\vartheta+Q_\vartheta^*, \tag{18}$$

where N_x^*, N_ϑ^*, M_x^*, M_ϑ^*, Q_x^* and Q_ϑ^* are related to the piezoelectric layers bonded on the host shell. Then, we can write:

$$N_x^*=-\int_{-\frac{H}{2}}^{-\frac{H_h}{2}} e_{31}E_z\left(1+\frac{z}{R}\right)dz-\int_{\frac{H_h}{2}}^{\frac{H}{2}} e_{31}E_z\left(1+\frac{z}{R}\right)dz,$$
$$N_\vartheta^*=-\int_{-\frac{H}{2}}^{-\frac{H_h}{2}} e_{32}E_z dz-\int_{\frac{H_h}{2}}^{\frac{H}{2}} e_{32}E_z dz,$$
$$M_x^*=-\int_{-\frac{H}{2}}^{-\frac{H_h}{2}} e_{31}E_z z\left(1+\frac{z}{R}\right)dz-\int_{\frac{H_h}{2}}^{\frac{H}{2}} e_{31}E_z z\left(1+\frac{z}{R}\right)dz,$$
$$M_\vartheta^*=-\int_{-\frac{H}{2}}^{-\frac{H_h}{2}} e_{32}E_z z dz-\int_{\frac{H_h}{2}}^{\frac{H}{2}} e_{32}E_z z dz,$$
$$Q_x^*=-\int_{-\frac{H}{2}}^{-\frac{H_h}{2}} K_{55}e_{15}E_x\left(1+\frac{z}{R}\right)dz$$
$$-\int_{\frac{H_h}{2}}^{\frac{H}{2}} K_{55}e_{15}E_x\left(1+\frac{z}{R}\right)dz,$$
$$Q_\vartheta^*=-\int_{-\frac{H}{2}}^{-\frac{H_h}{2}} K_{44}e_{24}E_\vartheta dz-\int_{\frac{H_h}{2}}^{\frac{H}{2}} K_{44}e_{24}E_\vartheta dz. \tag{19}$$

In the above equations, the first and second integrations correspond to the internal and external piezoelectric layers, respectively. Also, we have:

$$A_{ij}=\int_{-\frac{H}{2}}^{-\frac{H_h}{2}} K_{ij}^2C_{ij}dz+\int_{-\frac{H_h}{2}}^{\frac{H_h}{2}} K_{ij}^2Q_{ij}dz$$
$$+\int_{\frac{H_h}{2}}^{\frac{H}{2}} K_{ij}^2C_{ij}dz,$$
$$B_{ij}=\int_{-\frac{H}{2}}^{-\frac{H_h}{2}} K_{ij}^2C_{ij}zdz+\int_{-\frac{H_h}{2}}^{\frac{H_h}{2}} K_{ij}^2Q_{ij}zdz$$
$$+\int_{\frac{H_h}{2}}^{\frac{H}{2}} K_{ij}^2C_{ij}zdz,$$
$$C_{ij}=\int_{-\frac{H}{2}}^{-\frac{H_h}{2}} K_{ij}^2C_{ij}z^2dz+\int_{-\frac{H_h}{2}}^{\frac{H_h}{2}} K_{ij}^2Q_{ij}z^2dz$$
$$+\int_{\frac{H_h}{2}}^{\frac{H}{2}} K_{ij}^2C_{ij}z^2dz,$$
$$D_{ij}=\int_{-\frac{H}{2}}^{-\frac{H_h}{2}} K_{ij}^2C_{ij}z^3dz+\int_{-\frac{H_h}{2}}^{\frac{H_h}{2}} K_{ij}^2Q_{ij}z^3dz$$
$$+\int_{\frac{H_h}{2}}^{\frac{H}{2}} K_{ij}^2C_{ij}z^3dz,$$
$$E_{ij}=\int_{-\frac{H}{2}}^{-\frac{H_h}{2}} K_{ij}^2C_{ij}z^4dz+\int_{-\frac{H_h}{2}}^{\frac{H_h}{2}} K_{ij}^2Q_{ij}z^4dz$$
$$+\int_{\frac{H_h}{2}}^{\frac{H}{2}} K_{ij}^2C_{ij}z^4dz, \tag{20}$$

and $K_{ij}=1$, except for K_{44} and K_{55}. The shear correction factors are taken as $K_{44}=K_{55}=\sqrt{\frac{5}{6}}$ [36].

Substituting Eqs. (18) into the motion equations (Eqs. (1)) gives us the following partial differential equations in terms of the displacements:

$$\left(A_{11}+\frac{B_{11}}{R}+\frac{e_{31}^2}{\eta_{33}}(2H_p)\right)u_{0,xx}$$
$$+\left(\frac{A_{66}}{R^2}-\frac{B_{66}}{R^3}+\frac{C_{66}}{R^4}\right)u_{0,\vartheta\vartheta}$$
$$+\left(\frac{A_{12}}{R}+\frac{A_{66}}{R}+\frac{e_{31}e_{32}}{\eta_{33}}\left(\frac{2H_p}{R}\right)\right)v_{0,x\vartheta}$$
$$+\left(\frac{A_{12}}{R}+\frac{e_{31}e_{32}}{\eta_{33}}\left(\frac{2H_p}{R}\right)\right)w_{0,x}$$
$$+\left(B_{11}+\frac{C_{11}}{R}+\frac{e_{31}^2}{\eta_{33}}\frac{2}{3R}\left(\left(\frac{H}{2}\right)^3\right.\right.$$
$$\left.\left.-\left(\frac{H}{2}-H_p\right)^3\right)\right)\varphi_{x,xx}+\left(\frac{B_{66}}{R^2}-\frac{C_{66}}{R^3}+\frac{D_{66}}{R^4}\right)\varphi_{x,\vartheta\vartheta}$$
$$+\left(\frac{B_{12}}{R}+\frac{B_{66}}{R}+\frac{e_{31}e_{32}}{\eta_{33}}\frac{2}{3R^2}\left(\left(\frac{H}{2}\right)^3\right.\right.$$
$$\left.\left.-\left(\frac{H}{2}-H_p\right)^3\right)\right)\varphi_{\vartheta,x\vartheta}+P'_x=I_0\ddot{u}_0+I_1\ddot{\varphi}_x,$$

$$\left(\frac{A_{12}}{R}+\frac{A_{66}}{R}+\frac{e_{31}e_{32}}{\eta_{33}}\left(\frac{2H_p}{R}\right)\right)u_{0,x\vartheta}$$
$$-\left(\frac{A_{44}}{R^2}-\frac{B_{44}}{R^3}+\frac{C_{44}}{R^4}\right)v_0$$
$$+\left(A_{66}+\frac{B_{66}}{R}\right)v_{0,xx}$$
$$+\left(\frac{A_{22}}{R^2}-\frac{B_{22}}{R^3}+\frac{C_{22}}{R^4}+\frac{e_{32}^2}{\eta_{33}}\left(\frac{2H_p}{R^2}\right)\right)v_{0,\vartheta\vartheta}$$
$$+\left(\frac{A_{22}}{R^2}+\frac{A_{44}}{R^2}-\frac{B_{22}}{R^3}-\frac{B_{44}}{R^3}\right.$$
$$\left.+\frac{C_{22}}{R^4}+\frac{C_{44}}{R^4}+\frac{e_{32}^2}{\eta_{33}}\left(\frac{2H_p}{R^2}\right)\right)w_{0,\vartheta}$$
$$+\left(\frac{B_{12}}{R}+\frac{B_{66}}{R}\right)\varphi_{x,x\vartheta}$$
$$+\left(\frac{A_{44}}{R}-\frac{B_{44}}{R^2}+\frac{C_{44}}{R^3}\right)\varphi_{\vartheta}$$
$$+\left(B_{66}+\frac{C_{66}}{R}\right)\varphi_{\vartheta,xx}$$
$$+\left(\frac{B_{22}}{R^2}-\frac{C_{22}}{R^3}+\frac{D_{22}}{R^4}\right)\varphi_{\vartheta,\vartheta\vartheta}+P'_{\vartheta}=I_0\ddot{v}_0+I_1\ddot{\varphi}_{\vartheta},$$

$$\left(\frac{A_{12}}{R}+\frac{e_{31}e_{32}}{\eta_{33}}\left(\frac{2H_p}{R}\right)\right)u_{0,x}+\left(\frac{A_{22}}{R^2}+\frac{A_{44}}{R^2}\right.$$
$$\left.-\frac{B_{22}}{R^3}-\frac{B_{44}}{R^3}+\frac{C_{22}}{R^4}+\frac{C_{44}}{R^4}+\frac{e_{32}^2}{\eta_{33}}\left(\frac{2H_p}{R^2}\right)\right)v_{0,\vartheta}$$
$$+\left(\frac{A_{22}}{R^2}-\frac{B_{22}}{R^3}+\frac{C_{22}}{R^4}+\frac{e_{32}^2}{\eta_{33}}\left(\frac{2H_p}{R^2}\right)\right)w_0$$
$$-\left(A_{55}+\frac{B_{55}}{R}\right)w_{0,xx}-\left(\frac{A_{44}}{R^2}-\frac{B_{44}}{R^3}+\frac{C_{44}}{R^4}\right)w_{0,\vartheta\vartheta}$$
$$-\left(A_{55}-\frac{B_{12}}{R}+\frac{B_{55}}{R}\right)\varphi_{x,x}$$
$$-\left(\frac{A_{44}}{R}-\frac{B_{22}}{R^2}-\frac{B_{44}}{R^2}+\frac{C_{22}}{R^3}+\frac{C_{44}}{R^3}-\frac{D_{22}}{R^4}\right)\varphi_{\vartheta,\vartheta}$$
$$+P'_z=I_0\ddot{w}_0,$$

$$\left(B_{11}+\frac{C_{11}}{R}+\frac{e_{31}^2}{\eta_{33}}\frac{2}{3R}\left(\left(\frac{H}{2}\right)^3\right.\right.$$
$$\left.\left.-\left(\frac{H}{2}-H_p\right)^3\right)\right)u_{0,xx}$$
$$+\left(\frac{B_{66}}{R^2}-\frac{C_{66}}{R^3}+\frac{D_{66}}{R^4}\right)u_{0,\vartheta\vartheta}$$
$$+\left(\frac{B_{12}}{R}+\frac{B_{66}}{R}+\frac{e_{31}e_{32}}{\eta_{33}}\frac{2}{3R^2}\left(\left(\frac{H}{2}\right)^3\right.\right.$$
$$\left.\left.-\left(\frac{H}{2}-H_p\right)^3\right)\right)v_{0,x\vartheta}-\left(A_{55}-\frac{B_{12}}{R}+\frac{B_{55}}{R}\right.$$
$$\left.-\frac{e_{31}e_{32}}{\eta_{33}}\frac{2}{3R^2}\left(\left(\frac{H}{2}\right)^3-\left(\frac{H}{2}-H_p\right)^3\right)\right)w_{0,x}$$
$$-\left(A_{55}+\frac{B_{55}}{R}\right)\varphi_x+\left(C_{11}+\frac{D_{11}}{R}\right.$$
$$\left.+\frac{e_{31}^2}{\eta_{33}}\frac{2}{3}\left(\left(\frac{H}{2}\right)^3-\left(\frac{H}{2}-H_p\right)^3\right)\right)\varphi_{x,xx}$$
$$+\left(\frac{C_{66}}{R^2}-\frac{D_{66}}{R^3}+\frac{E_{66}}{R^4}\right)\varphi_{x,\vartheta\vartheta}$$
$$+(\frac{C_{12}}{R}+\frac{C_{66}}{R}+\frac{e_{31}e_{32}}{\eta_{33}}\frac{2}{3R}(\left(\frac{H}{2}\right)^3$$
$$-\left(\frac{H}{2}-H_p\right)^3))\varphi_{\vartheta,x\vartheta}+m'_x=I_1\ddot{u}_0+I_2\ddot{\varphi}_x,$$

$$\left(\frac{B_{12}}{R}+\frac{B_{66}}{R}\right)u_{0,x\vartheta}+\left(\frac{A_{44}}{R}-\frac{B_{44}}{R^2}+\frac{C_{44}}{R^3}\right)v_0$$

$$+\left(B_{66}+\frac{C_{66}}{R}\right)v_{0,xx}+\left(\frac{B_{22}}{R^2}-\frac{C_{22}}{R^3}+\frac{D_{22}}{R^4}\right)v_{0,\vartheta\vartheta}$$

$$-\left(\frac{A_{44}}{R}-\frac{B_{22}}{R^2}-\frac{B_{44}}{R^2}+\frac{C_{22}}{R^3}+\frac{C_{44}}{R^3}-\frac{D_{22}}{R^4}\right)w_{0,\vartheta}$$

$$+\left(\frac{C_{12}}{R}+\frac{C_{66}}{R}+\frac{e_{31}e_{32}}{\eta_{33}}\frac{2}{3R}\left(\left(\frac{H}{2}\right)^3\right.\right.$$

$$\left.\left.-\left(\frac{H}{2}-H_p\right)^3\right)\right)\varphi_{x,x\vartheta}-\left(A_{44}-\frac{B_{44}}{R}+\frac{C_{44}}{R^2}\right)\varphi_\vartheta$$

$$+\left(C_{66}+\frac{D_{66}}{R}\right)\varphi_{\vartheta,xx}+\left(\frac{C_{22}}{R^2}-\frac{D_{22}}{R^3}+\frac{E_{22}}{R^4}\right.$$

$$\left.+\frac{e_{32}^2}{\eta_{33}}\frac{2}{3R^2}\left(\left(\frac{H}{2}\right)^3-\left(\frac{H}{2}-H_p\right)^3\right)\right)\varphi_{\vartheta,\vartheta\vartheta}$$

$$+m'_\vartheta=I_1\ddot{v}_0+I_2\ddot{\varphi}_\vartheta, \tag{21}$$

where:

$$P'_x=P_x+N'_{x,x},\qquad P'_\vartheta=P_\vartheta+\frac{N'_{\vartheta,\vartheta}}{R},$$

$$P'_z=P_z-\frac{N'_\vartheta}{R},\qquad m'_x=m_x+M'_{x,x},$$

$$m'_\vartheta=m_\vartheta+\frac{M'_{\vartheta,\vartheta}}{R}. \tag{22}$$

2.5. Navier solution method

The Navier-type solutions which satisfy the simply supported boundary conditions are in the form of the following series:

$$(u_0,\varphi_x,Q_x,P_x,m_x)=\sum_{m,n=1}^{\infty}$$

$$(u_0,\varphi_x,Q_x,P_x,m_x)_{mn}(t)\cos\alpha x\cos\beta\vartheta,$$

$$(v_0,\varphi_\vartheta,Q_\vartheta,P_\vartheta,m_\vartheta)=\sum_{m,n=1}^{\infty}$$

$$(v_0,\varphi_\vartheta,Q_\vartheta,P_\vartheta,m_\vartheta)_{mn}(t)\sin\alpha x\sin\beta\vartheta,$$

$$(w_0,N_x,N_\vartheta,M_x,M_\vartheta,P_z)=\sum_{m,n=1}^{\infty}$$

$$(w_0,N_x,N_\vartheta,M_x,M_\vartheta,P_z)_{mn}(t)\sin\alpha x\cos\beta\vartheta,$$

$$(N_{x\vartheta},N_{\vartheta x},M_{x\vartheta},M_{\vartheta x})=\sum_{m,n=1}^{\infty}$$

$$(N_{x\vartheta},N_{\vartheta x},M_{x\vartheta},M_{\vartheta x})_{mn}(t)\cos\alpha x\sin\beta\vartheta, \tag{23}$$

where:

$$\alpha=\frac{m\pi}{L},\qquad \beta=\frac{n\pi}{\varphi}.$$

And now, by substituting Eqs. (23) into Eqs. (21), we obtain the following matrix equation:

$$[M]\begin{Bmatrix}\ddot{u}_{0mn}\\ \ddot{v}_{0mn}\\ \ddot{w}_{0mn}\\ \ddot{\varphi}_{xmn}\\ \ddot{\varphi}_{\vartheta mn}\end{Bmatrix}+[K]\begin{Bmatrix}u_{0mn}\\ v_{0mn}\\ w_{0mn}\\ \varphi_{xmn}\\ \varphi_{\vartheta mn}\end{Bmatrix}=\begin{Bmatrix}p_{1mn}\\ p_{2mn}\\ p_{3mn}\\ p_{4mn}\\ p_{5mn}\end{Bmatrix}, \tag{24}$$

where $[M]$, $[K]$ are the inertia and stiffness matrices, and $\{\ddot{U}\}$, $\{U\}$, $\{P\}$ are the acceleration, displacement and load vectors. The coefficients of matrix K are very complicated. They are computed using Maple software and not presented here.

3. Time integration

The Newmark family of methods is used in the present study to numerically time integrate the system of five coupled second order ODEs. The recursive relation among displacements, and velocities $t+\Delta t$, are:

$$u^{t+\Delta t}=u^t+\Delta t\dot{u}^t+\frac{\Delta t^2}{2}\left[(1-2\beta)\ddot{u}^t+2\beta\ddot{u}^{t+\Delta t}\right], \tag{25}$$

$$\dot{u}^{t+\Delta t}=\dot{u}^t+\Delta t\left[(1-\gamma)\ddot{u}^t+\gamma\ddot{u}^{t+\Delta t}\right]. \tag{26}$$

The Newmark's parameters are chosen to be $\beta=\frac{1}{4}$ and $\gamma=\frac{1}{2}$. By setting these parameters, it results in the constant acceleration scheme, which is desirable because of its second order accuracy and non-dissipative nature.

4. Results and discussion

4.1. Example 1

Consider a three-layered circular cylinder made of a two-layered cross ply graphite–epoxy laminate [0°/90°] and a PZT-4 layer bonded to its outer surface. All layers have equal thickness. In this example, the radius and length of the shell are $R = 1$ m and $L = 4$ m, respectively. The value of the thickness is $S = R/H = 10$. The material properties of the graphite-epoxy and the piezoelectric layers are listed in Tables 1 and 2.

The forcing function is chosen as:

$$P_z=P_0(1-e^{-13100t}),\qquad \phi_1=\phi_2=0. \tag{27}$$

Table 1. Material properties of the unidirectional fiber reinforced graphite/epoxy.

Young modulus (GPa)		Shear modulus (GPa)		Poisson's ratio	
E_L	E_T	G_{LT}	G_{TT}	ν_{LT}	ν_{TT}
172.5	6.9	3.45	1.38	0.25	0.25

Table 2. Material properties of piezoelectric layers.

Material	Elastic constants (GPa)								
	C_{11}	C_{12}	C_{13}	C_{22}	C_{23}	C_{33}	C_{44}	C_{55}	C_{66}
PZT	139.0	77.8	74.3	139.0	74.3	115.0	25.6	25.6	30.6

Material	Piezoelectric constants (C/m^2)					Permittivity (C^2/Nm^2 $\times 10^{-9}$)			Density (kg/m^3)
	e_{31}	e_{32}	e_{33}	e_{24}	e_{15}	η_{11}	η_{22}	η_{33}	ρ
PZT-4	15.7	-5.3	-5.3	12.7	12.7	6.46	6.46	5.62	7600

Table 3. Material properties of host shells.

Material	Mass density (kg/m^3)	Young's modulus (GPa)	Poisson's ratio
Aluminum	2.80×10^3	70	0.33
Copper	8.86×10^3	115	0.31
Mild steel	7.86×10^3	199.5	0.29

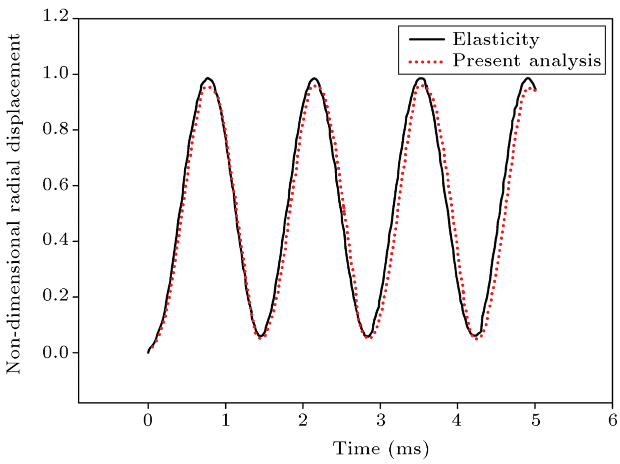

Figure 3. Variation of non-dimensional radial displacement versus time.

In order to compare with the results of the other studies, the maximum non-dimensional radial displacement is described in the following form:

$$w^* = \frac{100Y_T}{HS^4P_0}w. \tag{28}$$

The time history of the non-dimensional radial displacement in the inner surface of the shell is presented in Figure 3. Comparison of the results with those obtained from the three-dimensional elasticity solution [37,38] shows very good agreement.

4.2. Example 2

In this example, the displacements of a circular cylindrical shell covered with piezoelectric layers, with simply supported edges, are calculated. The material properties of piezoelectric layers and the host shell of steel are listed in Tables 2 and 3.

The value of the thickness is $S = R/H = 4$. The radius of the shell is 60 mm. The ratios of the thickness of the piezoelectric layers to the thickness of the host shell structure are chosen to be $H_p/H_H = 0.2$. The variation of the radial strains versus time for each case of loading is presented in Figure 4.

In order to validate the obtained results, a dynamic finite element solution for the same example is given by the authors. As shown in Figure 4, it can be seen that good agreement stands between the results, and deviations are negligible.

4.3. Example 3

In this example, the radial displacements of three simply supported cylinders covered with two piezoelectric layers on the inner and outer surfaces are calculated. The material properties of the host shells of aluminum, copper and steel are listed in Table 3. The material properties of the piezoelectric layers in this example are the same as in the previous one. The shells are under direct piezoelectric effects and there are no external applied voltages. The length and radius of the shell are equal to 8.25×10^{-2} m and 2.46×10^{-2} m, respectively.

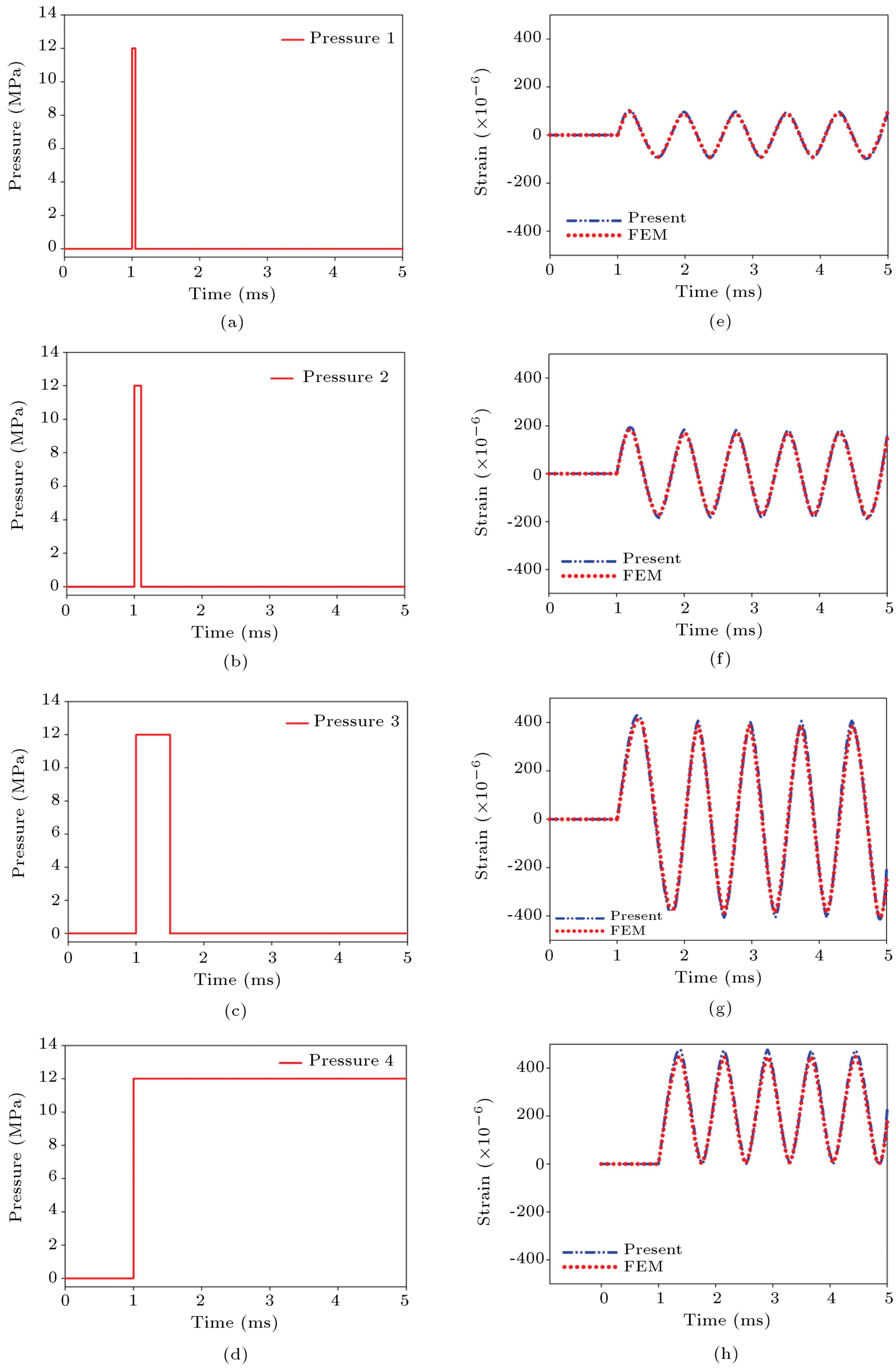

Figure 4. (a)-(d) Pressure-time graphs. (e)-(h) Strain-time graphs for each pressure.

Moreover, the values of the thickness, defined as $S = R/H$, are 2, 4 and 10.

The pressure acting on the shell surface is an electro-magnetic pressure, which is plotted in Figure 5. It can be seen that the duration of the applied pressure is about 80 ms. The non-dimensional radial displacement is defined as follows:

$$w^* = \frac{E}{HP_0}w, \tag{29}$$

where P_0 is the amplitude of the external pressure acting on the shell. Figures 6-8 show the non-dimensional

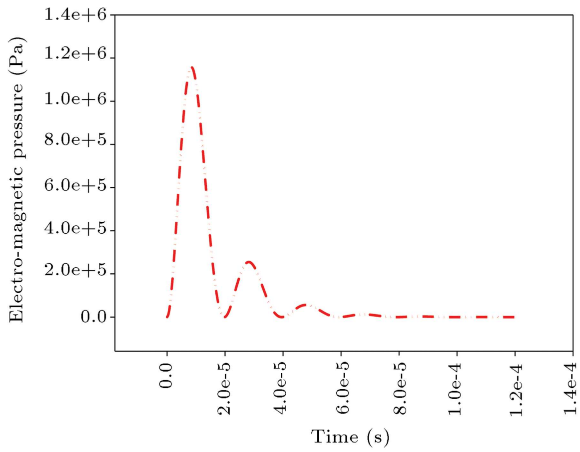

Figure 5. Variation of radial pressure versus time.

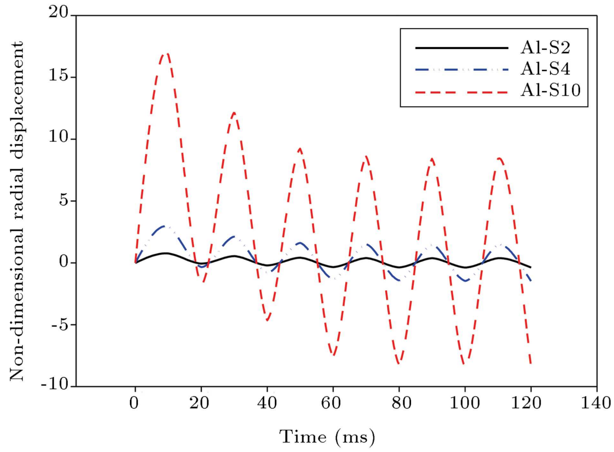

Figure 6. Non-dimensional radial displacement versus time for aluminum cylinder with $S = 2$, 4, 10 at (0, 0, $L/2$).

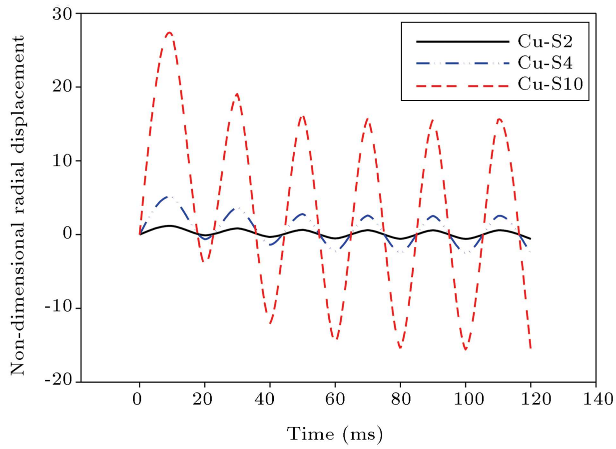

Figure 7. Non-dimensional radial displacement versus time for copper cylinder with $S = 2$, 4, 10 at (0, 0, $L/2$).

radial displacement versus time for aluminum, copper and steel cylinders with different thickness ratios. These figures represent the vibration behavior of the cylinders under the given dynamic load.

The results indicate that, under this loading

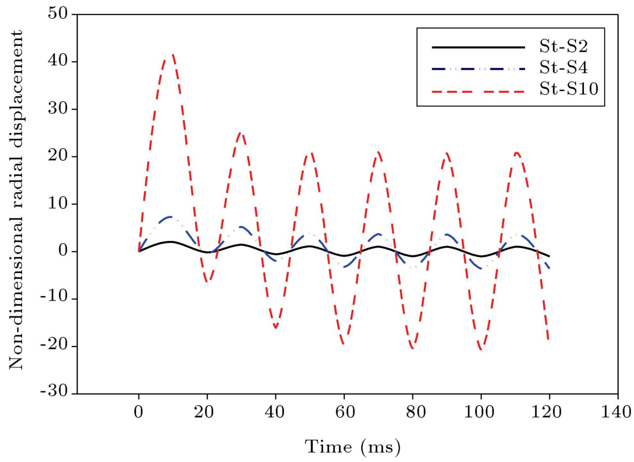

Figure 8. Non-dimensional radial displacement versus time for steel cylinder with $S = 2$, 4, 10 at (0, 0, $L/2$).

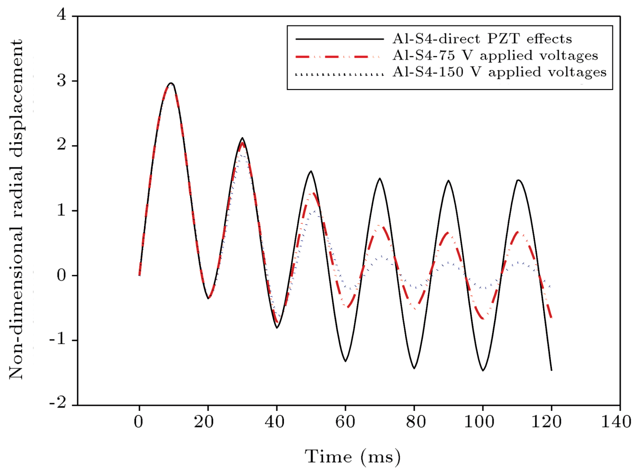

Figure 9. Non-dimensional radial displacement versus time for aluminum cylinder with $S = 4$, excited by different applied voltages.

condition, until $t = 80$ ms, the dynamic deflection of the cylinders goes up and down across the average magnitude of the pressure variations. When the pressure vanishes, there is a steady harmonic curve which moves up and down on the time axis.

Figure 9 illustrates the effects of the applied voltages on the vibration damping of an aluminum cylinder with surfaces bonded by PZT-4 layers. The plotted curves in this figure exhibit the direct piezoelectric effect and the mechanical response to the symmetric applied voltages (75 V and 150 V). It can be seen that with the decrease in magnitude of the external load, the effect of the applied actuation potential will be increased during the time period. These effects will be more apparent when the pressure vanishes.

5. Conclusion

In this paper, an investigation of the dynamic behavior of thick piezoelectric cylinders under different types of dynamic loading was presented. Five governing equations, in terms of resultant forces and resultant moments, were used in this investigation. The FSDT was developed, including the inertia, rotary inertia, stiffness and piezoelectric effects of the piezoelectric layers. The Navier solution was used for simply supported cylinders. The Newmark method was employed for time integration.

Three examples are provided in detail by the authors to illustrate the effectiveness of the presented method. Comparing the results of the presented method with those available in the literature shows satisfactory agreement. Also, different boundary conditions, host shell materials (which may be isotropic and orthotropic), ratios of the thickness of the host shell and piezoelectric layers, order of shear deformation theories and even forms of assumed solutions can be easily accommodated into the analysis. The results of this paper can serve as a reference for future study in the design of smart engineering structures.

References

1. Tiersten, H.F., *Linear Piezoelectric Plate Vibrations*, Plenum Press, New York (1969).
2. Tzou, H.S. and Zhong, J.P. "A linear theory of piezoelectric shell vibrations", *Journal of Sound and Vibration*, **175**, pp. 77-88 (1994).
3. Lee, C.K. "Theory of laminated piezoelectric plates for the design of distributed sensors/actuators. Part I: Governing equations and reciprocal relationships", *Journal of the Acoustical Society of America*, **87**, pp. 1144-1158 (1990).
4. Tzou, H.S. "A new distributed sensor and actuator theory for intelligent shell", *Journal of Sound and Vibration*, **152**, pp. 335-349 (1992).
5. Tzou, H.S. and Fu, H.Q. "A study of segmentation of distributed piezoelectric sensors and actuators. Part 1: Theoretical Analysis", *Journal of Sound and Vibration*, **172**, pp. 247-259 (1994).
6. Tzou, H.S. and Fu, H.Q. "A study of segmentation of distributed piezoelectric sensors and actuators. Part 2: Parametric study and active vibration controls", *Journal of Sound and Vibration*, **172**, pp. 261-275 (1994).
7. Tzou, H.S., Bou, Y. and Venkayya, V.B. "Parametric study of segmented transducers laminated on cylindrical shells. Part 1: Sensor patches", *Journal of Sound and Vibration*, **197**, pp. 207-224 (1996).
8. Tzou, H.S., Bou, Y. and Venkayya, V.B. "Parametric study of segmented transducers laminated on cylindrical shells. Part 2: Actuator patches", *Journal of Sound and Vibration*, **197**, pp. 225-249 (1996).
9. Pinto Correia, I.F., Mota Soares, C.M., Mota Soares, C.A. and Herskovits, J. "Active control of axisymmetric shells with piezoelectric layers: A mixed laminated theory with a high order displacement field", *Computers and Structures*, **80**, pp. 2265-2275 (2002).
10. Kapuria, S., Sengupta, S. and Dumir, P.C. "Three dimensional solution for simply supported piezoelectric cylindrical shell for axisymmetric load", *Computer Methods in Applied Mechanics and Engineering*, **140**, pp. 139-155 (1997).
11. Kapuria, S., Sengupta, S. and Dumir, P.C. "Three-dimensional piezothermoelastic solution for shape control of cylindrical panel", *Journal of Thermal Stresses*, **20**, pp. 67-85 (1997).
12. Kapuria, S., Sengupta S. and Dumir, P.C. "Assessment of shell theories for hybrid piezoelectric cylindrical shell under electromechanical load", *International Journal of Mechanical Sciences*, **40**, pp. 461-477 (1998).
13. Ray, M.C., Rao, K.M. and Samanta, B. "Exact analysis of coupled electrostatic behavior of a piezoelectric plate under cylindrical bending", *Computers and Structures*, **45**, pp. 667-677 (1992).
14. Dube, G.P., Kapuria, S. and Dumir, P.C. "Exact piezothermoelastic solution of simply-supported orthotropic flat panel in cylindrical bending", *International Journal of Mechanical Sciences*, **38**, pp. 1161-1177 (1996).
15. Chen, C.Q., Shen Y.P. and Wang, X.M. "Exact solution for orthotropic cylindrical shell with piezoelectric layers under cylindrical bending", *International Journal of Solids and Structures*, **33**, pp. 4481-4494 (1996).
16. Heyliger, P. "A note on the static behaviour of simply-supported laminated piezoelectric cylinders", *International Journal of Solids and Structures*, **34**, pp. 3781-3794 (1997).
17. Darvizeh, M., Darvizeh, A., Arab Zadeh, V. and Rajabi, H. "Nonlinear analysis of multi-layered beams with piezoelectric layers considering large deformations", *The Modares Journal of Mechanical Engineering*, **10**(2), pp. 57-68 (2010).
18. Shakeri, M., Eslami, M.R. and Daneshmehr, A. "Dynamic analysis of thick laminated shell panel with piezoelectric layer based on three dimensional elasticity solution", *Computers and Structures*, **84**, pp. 1519-1526 (2006).
19. Darvizeh, M., Haftchenari, H., Darvizeh, A., Ansari, R. and Alijani, A. "The effect of piezoelectric on buckling behavior of composite cylinders", In *The Proceedings of the WSEAS Transactions on Information science and Applications*, Yokohama, Japan, pp. 1195-1201 (2005).
20. Rajabi, H., Rezaei, A., Darvizeh, A. and Darvizeh, M. "Analytical analysis of thick-walled tubes coated with piezoelectric layers under dynamic loading", In *The Proceedings of the Asian Pacific Conference on Materials and Mechanics*, pp. 201- 205 (2009).
21. Rajabi, H., Darvizeh, A., Fallah Nejad, Kh. and Khaheshi, A. "Dynamic response of piezoelectric circular cylinders to internal dynamic loading", In *The*

Proceedings of the International Conference on Applied Mechanics, Materials and Manufacturing, Muscat, Oman, pp. 36-42 (2010).

22. Hong, C.C. "Computational approach of piezoelectric shells by the GDQ method", *Composite Structures*, **92**(3), pp. 811-816 (2010).
23. Kumar, R., Mishra, B.K. and Jain, S.C. "Static and dynamic analysis of smart cylindrical shell", *Finite Elements in Analysis and Design*, **45**, pp. 13-24 (2008).
24. Klinkel, S. and Wagner, W. "A piezoelectric solids shell element based on a mixed variational formulation for geometrically linear and nonlinear applications", *Computers and Structures*, **86**, pp. 38-46 (2008).
25. Santos, H., Mota Soares, C.M., Mota Soares, C.A. and Reddy, J.N. "A finite element model for the analysis of 3D axisymmetric laminated shells with piezoelectric sensors and actuators", *Composite Structures*, **75**, pp. 170-178 (2006).
26. Santos, H., Mota Soares, C.M., Mota Soares, C.A. and Reddy, J.N. "A finite element model for the analysis of 3D axisymmetric laminated shells with piezoelectric sensors and actuators: Bending and free vibrations", *Computers and Structures*, **86**, pp. 940-947 (2008).
27. Deu, J.F., Larbi, W. and Ohayon, R. "Piezoelectric structural acoustic problems: Symmetric variational formulations and finite element results", *Computer Methods in Applied Mechanics and Engineering*, **197**, pp. 1715-1724 (2008).
28. Darvizeh, A. and Darvizeh, M., *Stress Analysis in Thick Spherical and Cylindrical Shells*, The University of Guilan Press, Rasht (1993).
29. Farshad, M., *Design and Analysis of Shell Structures*, Kluwer Academic Publishers, Boston (1992).
30. Grigorenko, A. "Investigation of static and dynamic behavior of anisotropic inhomogeneous shallow shells by spline approximation method", *Journal of Civil Engineering and Management*, **15**, pp. 1392-3730 (2009).
31. Ikeda, T., *Fundamental of Piezoelectricity*, Oxford University Press, Oxford (1996).
32. Dube, G.P., Dumir, P.C. and Kumar, C.B. "Segmented sensors and actuators for thick plates and shells. Part I: Analysis using FSDT", *Journal of Sound and Vibration*, **226**, pp. 739-753 (1999).
33. Hwu, C., Chang, W.C. and Gai, H.S. "Vibration suppression of composite sandwich beams", *Journal of Sound and Vibration*, **272**(1), pp. 1-20 (2004).
34. Balamurugan, V. and S. Narayanan "Shell finite element for smart piezoelectric composite plate/shell structures and its application to the study of active vibration control", *Finite Elements in Analysis and Design*, **37**(9), pp. 713-738 (2001).
35. Zhang, X.M. and Greenleaf, J.F. "An anisotropic model for frequency analysis of arterial walls with the wave propagation approach", *Applied Acoustics*, **68**, pp. 953-969 (2007).
36. Jonnalaggada, K.D., Blandford, G.E. and Tauchert, T.R. "Piezothermoelastic composite plate analysis using first-order shear deformation theory", *Computers and Structures*, **51**, pp. 79-89 (1994).
37. Shakeri, M., Yas, M.H. and Saviz, M.R. "Elasticity solution for laminated cylindrical shell with piezoelectric layer", In *The Proceedings of the International Conference on Recent Advances in Composite Materials*, Varanasi, India, pp. 519-526 (2004).
38. Yas, M.H., Shakeri, M. and Saviz, M.R. "Elasticity solution for laminated cylindrical shell with piezoelectric layer under local ring load", *Journal of Key Engineering Materials*, **334-335**, pp. 917-920 (2007).

Biographies

Hamed Rajabi received his BS and MS degrees in Mechanical Engineering in 2007 and 2010, respectively, from the University of Guilan, Iran, where he is currently a PhD degree student. His research interests include biomimetics, mechanics of biological tissues and materials, sustainability in engineering design and applied mechanics. He is author of more than 34 journal and conference papers.

Abolfazl Darvizeh received his MS and PhD degrees in Mechanical Engineering from the University of Manchester, Institute of Science and Technology (UMIST), UK, in 1979 and 1982, respectively. He was selected as Distinguished Professor of Iran by the Ministry of Science, Research and Technology, and, also, in Mechanical Engineering by the Iranian Society of Mechanical Engineering (ISME), in 1996 and 2006, respectively. He is author of 16 text books and more than 250 journal and conference papers. His teaching and research interests include biomimetic engineering, impact mechanics and high energy rate forming processes.